The activation of ezrin–radixin–moesin proteins is regulated by netrin-1 through Src kinase and RhoA/Rho kinase activities and mediates netrin-1–induced axon outgrowth

Judith Antoine-Bertrand, Atefeh Ghogha, Vilayphone Luangrath, Fiona K. Bedford, and Nathalie Lamarche-Vane
Department of Anatomy and Cell Biology, McGill University, Montreal H3A 2B2, PQ, Canada

ABSTRACT **The receptor Deleted in Colorectal Cancer (DCC) mediates the attractive response of axons to the guidance cue netrin-1 during development. On netrin-1 stimulation, DCC is phosphorylated and induces the assembly of signaling complexes within the growth cone, leading to activation of cytoskeleton regulators, namely the GTPases Rac1 and Cdc42. The molecular mechanisms that link netrin-1/DCC to the actin machinery remain unclear. In this study we seek to demonstrate that the actin-binding proteins ezrin–radixin–moesin (ERM) are effectors of netrin-1/DCC signaling in embryonic cortical neurons. We show that ezrin associates with DCC in a netrin-1–dependent manner. We demonstrate that netrin-1/DCC induces ERM phosphorylation and activation and that the phosphorylation of DCC is required in that context. Moreover, Src kinases and RhoA/Rho kinase activities mediate netrin-1–induced ERM phosphorylation in neurons. We also observed that phosphorylated ERM proteins accumulate in growth cone filopodia, where they colocalize with DCC upon netrin-1 stimulation. Finally, we show that loss of ezrin expression in cortical neurons significantly decreases axon outgrowth induced by netrin-1. Together, our findings demonstrate that netrin-1 induces the formation of an activated ERM/DCC complex in growth cone filopodia, which is required for netrin-1–dependent cortical axon outgrowth.**

Monitoring Editor
Kozo Kaibuchi
Nagoya University

Received: Nov 24, 2010
Revised: Jul 27, 2011
Accepted: Aug 5, 2011

INTRODUCTION

During the development of the CNS, extracellular cues guide axons to the appropriate cellular target. At the budding periphery of axons, the neuronal growth cone integrates attractive and repulsive sensory cues and translates them into the appropriate response (Guan and Rao, 2003; Lowery and Van Vactor, 2009). The GTPases Rac1, Cdc42, and RhoA, members of the Rho family of small GTPases, are major intracellular signaling molecules regulated downstream of most, if not all, axon guidance cues, including the netrins, ephrins, semaphorins, and slits (Huber *et al.*, 2003; Govek *et al.*, 2005; O'Donnell *et al.*, 2009). In the context of axon outgrowth and guidance, Rho GTPases drive the cytoskeletal rearrangements that mediate processes such as membrane protrusion or retraction, axonal shaft consolidation, and receptor endocytosis (Lowery and Van Vactor, 2009; Hall and Lalli, 2010).

Netrins are conserved bifunctional axon guidance molecules that can either attract or repel growing axons, depending on the nature of the neuron (Rajasekharan and Kennedy, 2009). In vertebrates, netrin-1 attracts and promotes the growth of a wide variety of neuronal cell types, including cortical and spinal commissural neurons (Kennedy *et al.*, 1994; Metin *et al.*, 1997; Richards *et al.*, 1997). The receptor Deleted in Colorectal Cancer (DCC) mediates the attractive responses induced by netrin-1 and is expressed in the spinal cord and the forebrain (Keino-Masu *et al.*, 1996; Shu *et al.*, 2000). A deficiency in either netrin-1 or DCC expression prevents the formation of spinal and cerebral commissures (Serafini *et al.*, 1996; Fazeli *et al.*, 1997). In recent years, the signaling cascade

This article was published online ahead of print in MBoC in Press (http://www.molbiolcell.org/cgi/doi/10.1091/mbc.E10-11-0917) on August 17, 2011.

Address correspondence to: Nathalie Lamarche-Vane (nathalie.lamarche@mcgill.ca).

Abbreviations used: DCC, Deleted in Colorectal Cancer; DIV, days of culture in vitro; ERM, ezrin–radixin–moesin; FERM, four-point one, ezrin, radixin, moesin; GFP, green fluorescent protein; pERM, phosphorylated ERM protein; SEM, standard error of the mean; GST, glutathione *S*-transferase; IgG, immunoglobulin G; TRITC, tetramethyl rhodamine isothiocyanate.

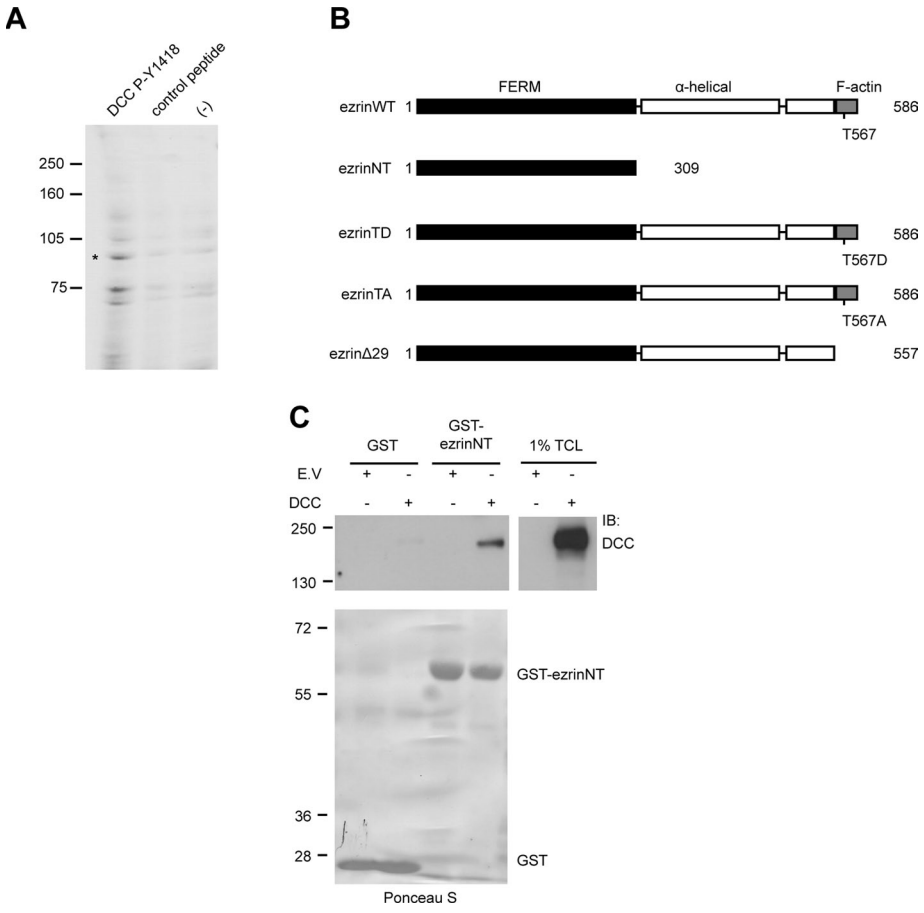

FIGURE 1: Ezrin interacts with DCC. (A) E13 rat brain protein lysates were incubated with Affi-Gel-DCC-P-Y1418 phosphopeptide, Affi-Gel-DCC unphosphorylated peptide (control), or Affi-Gel beads (−). Bound proteins were resolved by SDS–PAGE and stained with Coomassie blue. Peptides matching the ERM protein sequences of ezrin, radixin, and moesin were identified by MS/MS analysis of the band at approximately 85 kDa represented by the asterisk. (B) The domain architecture of wild-type ezrin (ezrinWT) and ezrin mutant proteins. EzrinWT consists of the N-terminal FERM domain, the α-helical linker region, and the C-terminal F-actin–binding domain. (C) Lysates of HEK293 cells transfected with pRK5 or pRK5-DCC were incubated with GST or GST-ezrinNT fusion proteins coupled to glutathione–agarose beads (n = 4). GST pull-down–associated proteins and 1% of total cell lysates (TCL) were resolved by SDS–PAGE and immunoblotted (IB) with antibodies against DCC. Purified GST proteins were stained with Ponceau S prior to immunoblotting (bottom).

regulated by netrin-1 and DCC has been extensively studied. Netrin-1 induces the phosphorylation of DCC on tyrosine, serine, and threonine residues (Meriane *et al.*, 2004). Src kinase activity and netrin-1–dependent phosphorylation of the C-terminal tyrosine residue 1418 (Y1418) of DCC are essential to netrin-1–mediated axon outgrowth and attraction (Li *et al.*, 2004; Meriane *et al.*, 2004; Ren *et al.*, 2008). Ultimately, netrin-1/DCC signal transduction leads to Rac1 and Cdc42 activation (Li *et al.*, 2002; Shekarabi and Kennedy, 2002), whereas RhoA activity is inhibited (Moore *et al.*, 2008). Although the F-actin regulators N-WASP and ADF/cofilin have been implicated in netrin-1 signaling (Shekarabi *et al.*, 2005; Marsick *et al.*, 2010), the regulation of actin-binding proteins in the context of netrin-1/DCC signaling is still poorly understood. The ezrin–radixin–moesin (ERM) proteins are conserved molecules that bridge the plasma membrane with the actin cytoskeleton. They share a similar domain structure that is characterized by an N-terminal four-point one, ezrin, radixin, moesin (FERM) domain, an α-helical linker region, and a C-terminal F-actin–binding domain (Fehon *et al.*, 2010). In the cytoplasm, the phosphorylation of a conserved C-terminal threonine residue is a crucial step in the activation of ERM proteins (Gary and Bretscher, 1995; Gautreau *et al.*, 2000; Fievet *et al.*, 2004). On phosphorylation, activated ERM proteins translocate from the cytoplasm to the plasma membrane, where their FERM domain binds to membrane-associated proteins such as cell-surface receptors (McClatchey and Fehon, 2009). Through their affinity for F-actin and their recruitment to the cell cortex, ERM proteins create an interface between transmembrane receptors and the cortical actin network (Charrin and Alcover, 2006; Niggli and Rossy, 2008; Fehon *et al.*, 2010). ERM proteins, including the brain-specific homologue merlin, are expressed during the development of the CNS (spinal cord and brain) in mouse and rat embryos (Paglini *et al.*, 1998; Kikuchi *et al.*, 2002; Ramesh, 2004; Saotome *et al.*, 2004). In primary embryonic neurons, ERM protein activity is associated with growth cone dynamics, neurite outgrowth, and branching (Paglini *et al.*, 1998; Cheng *et al.*, 2005; Haas *et al.*, 2007)

Here we demonstrate that ERM proteins are effectors of netrin-1/DCC signaling in embryonic cortical neurons. We show that ezrin interacts with DCC in a netrin-1–dependent manner. In response to netrin-1/DCC stimulation, ERM proteins are phosphorylated and activated in cortical neurons. Furthermore, we show that Src kinases and RhoA/Rho kinase activities are required for netrin-1 to mediate ERM activation. In addition, netrin-1 induces the accumulation of phosphorylated ERM proteins (pERMs) in growth cone filopodia, where they colocalize with the receptor DCC. Finally, impairing ERM activity inhibits DCC-mediated neurite outgrowth in mouse N1E-115 neuroblastoma cells, and loss of ezrin expression blocks netrin-1–induced axon outgrowth in primary cortical neurons. Together, these results show that netrin-1 induces the formation of a pERM–DCC complex in growth cone filopodia and that this complex is required for netrin-1–dependent cortical axon outgrowth.

RESULTS

Netrin-1 regulates the interaction of ezrin with DCC in embryonic cortical neurons

We previously demonstrated that DCC is phosphorylated by the Src kinase Fyn on Y1418 and that this phosphorylation is required to mediate Rac1 activation and neurite outgrowth (Meriane *et al.*, 2004). To identify proteins that interact with phosphorylated Y1418, we incubated embryonic day 13 (E13) rat brain protein lysates with Affi-Gel beads coupled to a 15–amino acid DCC peptide phosphorylated on Y1418 or to an unphosphorylated control peptide (Figure 1A). The bound proteins were resolved by SDS–PAGE and stained with Coomassie blue (Figure 1A). Tandem mass spectrometry (MS/MS) analysis performed on one band of ~85 kDa (Figure 1A, asterisk), which was enriched after incubation with the DCC

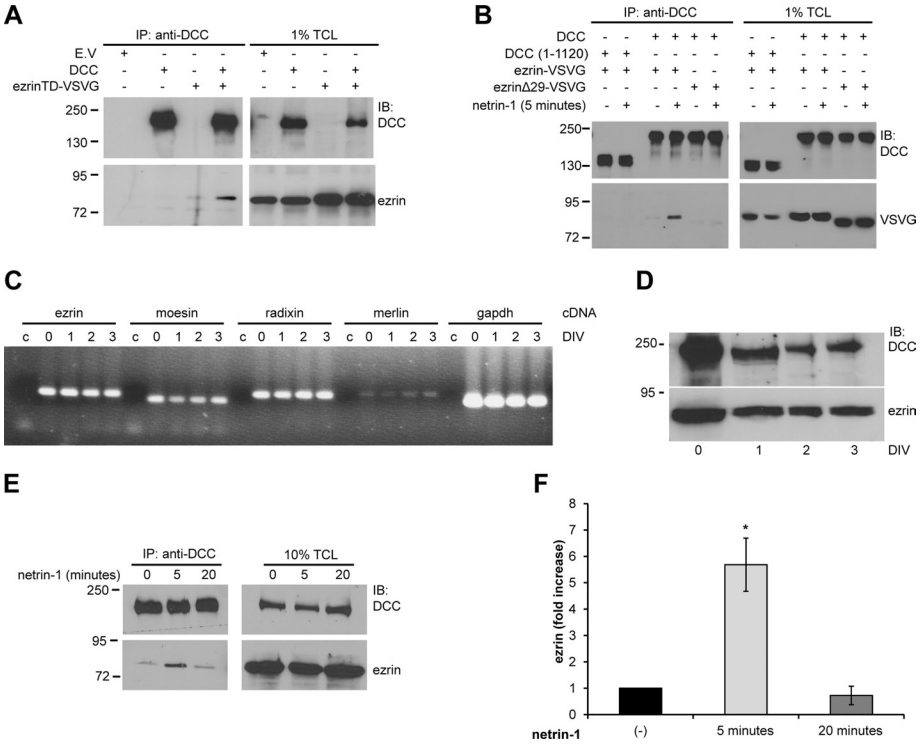

FIGURE 2: Netrin-1 regulates the interaction between ezrin and DCC. Protein lysates of N1E-115 cells (A) and HEK293 cells (B) transfected with empty vector (E.V.), pRK5-DCC, pRK5-DCC (1–1120), VSVG-tagged ezrinTD, ezrin wild type, or ezrinΔ29 as indicated or (E) lysates of embryonic rat cortical neurons (E18, 2DIV) stimulated with netrin-1 for various periods of time were submitted to immunoprecipitation (IP) using anti-DCC antibodies. Immunoprecipitated proteins and 1% (A, B) or 10% (E) of total cell lysates (TCL) were resolved by SDS–PAGE, followed by immunoblotting (IB) using anti-DCC, anti-ezrin, or anti-VSVG antibodies. mRNA (C) or proteins (D) were extracted from E18 cortices (0DIV) or cultured cortical neurons (1, 2, and 3 DIV). (C) RT-PCR amplification of cDNA from ezrin (233 base pairs), moesin (205 base pairs), radixin (242 base pairs), merlin (248 base pairs), and GAPDH (207 base pairs). Control reactions (c) were performed with water instead of cDNA for each primer pair. (D) Protein lysates of cortical neurons were resolved by SDS–PAGE and immunoblotted with antibodies against DCC or ezrin. (F) Quantitative densitometry of the amount of ezrin immunoprecipitated with DCC in E represented as the fold increase relative to unstimulated neurons (n = 3). The increase in the amount of ezrin immunoprecipitated is significant after 5 min of netrin-1 stimulation (*p < 0.01).

phosphopeptide, yielded four peptides corresponding to the ERM proteins ezrin, radixin, and moesin. The domain architecture of ezrin is characterized by the N-terminal FERM domain, the α-helical linker region, and the C-terminus, which harbors the actin-binding domain (Figure 1B). Because ERM proteins associate with proteins found at the plasma membrane via their FERM domain (Fehon *et al.*, 2010), we first determined whether the FERM domain of ezrin (ezrinNT) could interact with DCC in vitro by glutathione *S*-transferase (GST) pull-down assays. Indeed, the FERM domain of ezrin expressed as a GST fusion protein was found to interact with DCC overexpressed in HEK293 cells (Figure 1C). To further characterize the interaction, DCC was coexpressed with the constitutively active mutant protein ezrinT567D (ezrinTD) in N1E-115 cells, and a mouse monoclonal antibody against the extracellular domain of DCC was used to immunoprecipitate DCC from protein lysates. As shown in Figure 2A, VSVG-tagged ezrinT567D was able to coimmunoprecipitate with DCC. When ezrin was coexpressed with DCC in HEK293 cells stimulated with netrin-1, we observed that ezrin was able to interact with DCC in a netrin-1–dependent manner (Figure 2B). However, DCC lacking the intracellular domain (DCC (1–1120)) or inactive ezrin lacking the F-actin binding domain (ezrinΔ29) abolished the ezrin–DCC interaction (Figure 2B). These results confirm that the intracellular domain of DCC and the F-actin–binding domain of ezrin (including T567) are required to promote netrin-1–induced recruitment of ezrin to DCC in HEK293 cells. We next determined whether endogenous ezrin and DCC associate in embryonic cortical neurons. We first confirmed by reverse transcription (RT)-PCR that E18 cortical neurons cultured for 0–3 d in vitro (DIV) express ezrin mRNA and found that all three ERM mRNAs, as well as their brain-specific homologue merlin, were expressed (Figure 2C). The protein expression of DCC and ezrin was also confirmed by immunoblot (Figure 2D). In rat E18 cortical neurons at 2DIV, netrin-1 transiently stimulated the interaction of ezrin and DCC (Figure 2E). Coimmunoprecipitation of ezrin with DCC was observed after 5 min of netrin-1 stimulation and was significantly reduced after a 20-min stimulation (Figure 2, E and F). Only 0.26% of the total amount of DCC expressed in HEK293 cells was found to interact with GST-ezrinNT (Figure 1C), whereas the interaction of ezrin with DCC was increased by sixfold after stimulation of cortical neurons with netrin-1 (Figure 2F). Together, these results show that ezrin interacts with DCC via its FERM domain, that netrin-1 positively regulates the assembly of ezrin–DCC protein complexes in embryonic cortical neurons, and that this interaction is weak in the absence of netrin-1.

Netrin-1/DCC induces ERM phosphorylation in embryonic cortical neurons

Next we wanted to assess whether netrin-1 and DCC regulate the activation of ERM proteins in neurons. The activation state of ERM proteins in cell lysates was monitored by immunoblotting against pERMs using a phospho-specific ERM antibody that recognizes the phosphorylated form of the conserved C-terminal threonine residue in all three ERM proteins (Figure 1B). In embryonic cortical neurons stimulated with netrin-1 for different periods of time, we found that netrin-1 stimulation increased pERM levels after 5 min of stimulation (Figure 3A). There was a significant activation peak in ERM phosphorylation between 5 and 10 min of stimulation, with pERM/ezrin ratios of 1.94 ± 0.43 and 1.67 ± 0.09, respectively (Figure 3B). Past 10 min of netrin-1 stimulation, ERM phosphorylation decreased but appeared to be maintained. To confirm that DCC mediates the regulation of ERM proteins by netrin-1, dissociated embryonic cortical neurons were incubated with a function-blocking DCC antibody or with mouse immunoglobulin G (IgG) as a negative control prior to netrin-1 stimulation. Blocking the function of DCC resulted in the inhibition of netrin-1–mediated ERM phosphorylation in cortical neurons (Figure 3, C and D), thus confirming that DCC is required for netrin-1 to mediate ERM phosphorylation.

The phosphorylation of DCC on Y1418 has previously been shown to be important for netrin-1/DCC signaling (Li *et al.*, 2004; Meriane *et al.*, 2004; Ren *et al.*, 2008). In addition, we found that a

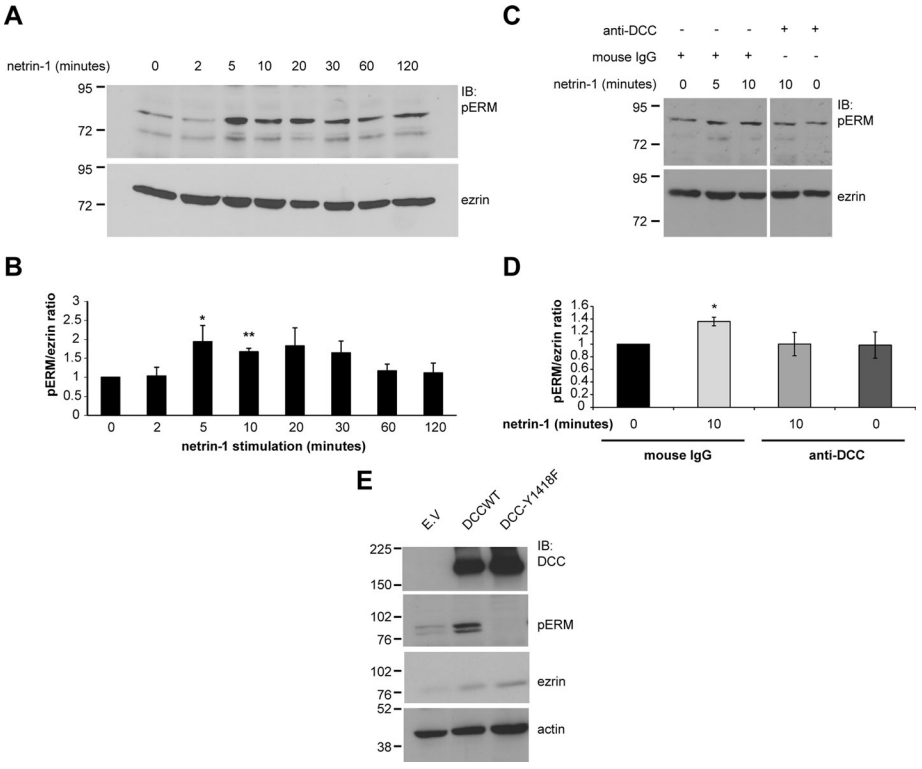

FIGURE 3: Netrin-1 induces the phosphorylation of ERM proteins through DCC in embryonic cortical neurons. (A) Protein lysates of embryonic rat cortical neurons (E18, 2DIV) stimulated with netrin-1 for various periods of time or (E) protein lysates of NIE-115 cells transfected with empty vector (E.V.), pRK5-DCC, or pRK5-DCC-Y1418F were resolved by SDS–PAGE, followed by immunoblotting using anti-DCC, anti-pERM, anti-ezrin, or anti-actin antibodies. (B) Quantitative densitometry of A is represented as the ratio of pERM over total ezrin and corresponds to the average of at least three independent experiments. The increase in pERM levels after 5 and 10 min of netrin-1 stimulation was significant (*$p < 0.05$; **$p < 0.005$). (C) The experiment was as described in A, except that function-blocking DCC antibodies were added before netrin-1 stimulation. Mouse IgGs were used as a negative control. (D) Quantitative densitometry of C is represented as the ratio of pERM over total ezrin and corresponds to the average of at least three independent experiments. The increase in pERM after 10 min of netrin-1 stimulation is significant (*$p < 0.05$). Error bars, SEM. (E) The upper pERM band represents ezrin and radixin, and the lower band is moesin.

DCC-Y1418 phosphopeptide was able to recruit ERM proteins in embryonic rat brain protein lysates (Figure 1A). Thus we examined whether the phosphorylation state of DCC-Y1418 influences pERM levels in N1E-115 cells, which endogenously express netrin-1 (Li *et al.*, 2002). We found that the expression of wild-type DCC in these cells increased significantly the phosphorylation of ERM proteins, whereas the expression of the phospho-deficient mutant DCC-Y1418F led to a reduction in ERM phosphorylation below the basal pERM levels observed in control cells transfected with empty vector (Figure 3E). Taken together, these results suggest that netrin-1 induces DCC-dependent ERM phosphorylation in cortical neurons and that the phosphorylation of DCC on Y1418 is required for netrin-1–mediated activation of ERM proteins.

Src kinases and RhoA/Rho kinase activities are required for netrin-1/DCC to mediate ERM activation

Axon outgrowth and guidance mediated by netrin-1/DCC signaling require the function of Src family kinases (Li *et al.*, 2004; Liu *et al.*, 2004; Meriane *et al.*, 2004; Ren *et al.*, 2008). To determine whether Src kinases also regulate ERM phosphorylation in response to netrin-1, embryonic cortical neurons were treated with netrin-1 in the presence of the Src kinase inhibitor PP2 or dimethyl sulfoxide (DMSO) as a control. Under these conditions, netrin-1 could no longer induce ERM phosphorylation in PP2-treated cortical neurons (Figure 4, A and B).

Rho GTPases promote ERM phosphorylation in neuronal and nonneuronal cells (Nakamura *et al.*, 2000; Haas *et al.*, 2007; Jeon *et al.*, 2010; Kim *et al.*, 2010). In addition, netrin-1 was found to regulate Rho GTPase activities in the mammalian brain and spinal cord (Li *et al.*, 2002; Briancon-Marjollet *et al.*, 2008; Moore *et al.*, 2008). The requirement for Rho GTPase activity in netrin-1–mediated ERM phosphorylation was first evaluated by inhibiting the activity of RhoA, Rac1, and Cdc42 with toxin B in cortical neurons (Figure 4C). The toxin B treatment significantly reduced the ability of netrin-1 to induce ERM phosphorylation (pERM/ezrin ratio, 1.21 ± 0.15) compared with the pERM levels observed with the control PBS treatment (pERM/ezrin ratio, 2.74 ± 0.44; Figure 4, C and D). Toxin B treatment did not influence ERM phosphorylation in unstimulated cortical neurons, thus confirming that the inhibitory effect observed with toxin B is specific to netrin-1–induced ERM phosphorylation. We next determined the specific contribution of RhoA, Rac1, and Cdc42 in the context of ERM phosphorylation by inhibiting RhoA or Rac1 activities with C3 transferase (C3T) and the NSC23766 compound, respectively, or by down-regulation of Cdc42 expression with synthetic siRNA targeting Cdc42. The inhibition of Rac1 by NSC23766 treatment or depletion of Cdc42 did not inhibit netrin-1–dependent ERM phosphorylation in cortical neurons (Supplemental Figure S1). On the other hand, the inhibition of RhoA by C3 transferase treatment was sufficient to block ERM phosphorylation induced by netrin-1 without altering the basal level of ERM phosphorylation in unstimulated cortical neurons (Figure 4, E and F). Furthermore, the inhibition of Rho kinase by Y27632 treatment also interfered with the ability of netrin-1 to induce ERM phosphorylation (Figure 4, G and H). Therefore these data demonstrate that the activities of Src kinases and RhoA/Rho kinase are solicited downstream of netrin-1 and DCC to mediate ERM phosphorylation.

Netrin-1 induces the accumulation of pERMs and their colocalization with DCC in neuronal growth cones

We next examined the localization of activated ERM proteins in netrin-1–stimulated cortical neurons by immunostaining neurons with antibodies specific for pERM. In unstimulated cortical neurons, pERMs were mostly localized in the filopodia emanating from neuronal cell bodies and practically absent from axons or growth cones (Figure 5A). After 5 and 20 min of netrin-1 stimulation, the pERM immunostaining was clearly increased (Figure 5A), which is reminiscent of the increase in pERM levels observed in cortical neuron lysates (Figure 3B). Netrin-1 induced a significant accumulation of pERM in growth cones compared with unstimulated neurons (Figure 5A), whereas no significant difference was observed for the ezrin

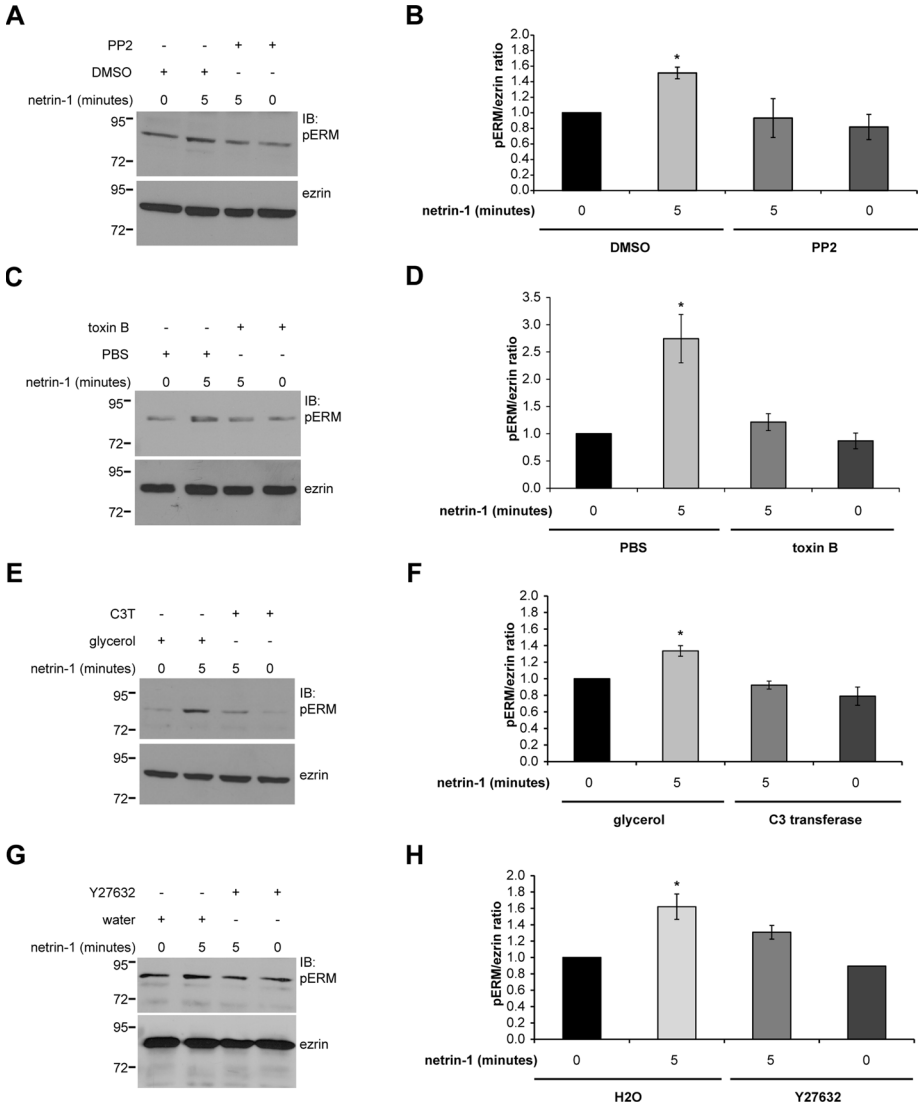

FIGURE 4: Src family kinases and RhoA/Rho kinase mediate ERM protein phosphorylation in cortical neurons stimulated with netrin-1. Embryonic rat cortical neurons (E18, 2DIV) were incubated with netrin-1 for the indicated times following treatment with (A, B) Src kinase inhibitor PP2 or DMSO as a negative control, (C, D) Rho GTPase inhibitor toxin B or PBS as a negative control, (E, F) RhoA inhibitor C3 transferase (C3T) or glycerol as a negative control, or (G, H) Rho kinase inhibitor Y27632 or water (H_2O) as a negative control. Protein lysates were resolved by SDS–PAGE and immunoblotted with anti-pERM or anti-ezrin antibodies. Quantitative densitometry is represented as the ratio of pERM over total ezrin and corresponds to the average of at least three independent experiments. The increase in pERM after 5 min of netrin-1 stimulation was significant (*$p < 0.05$), whereas there was no significant increase after the PP2, toxin B, C3 transferase, or Y27632 treatment compared with unstimulated neurons (0 min). Error bars, SEM.

immunostaining (Supplemental Figure S2A). When images of the pERM and DCC immunostainings were merged, colocalization between pERM and DCC was observed in growth cones after 5 and 20 min of stimulation with netrin-1 and not in unstimulated neurons (Figure 5, A and B). Moreover, netrin-1–induced pERM-DCC colocalization appeared to be restricted to the tips of the neuronal growth cones, in filopodia (Figure 5B). However, the level of pERM–DCC colocalization induced by netrin-1 was variable after 20 min of stimulation (Figure 5B, a and b), an observation that was confirmed when Pearson's correlation was used to quantify pERM–DCC colocalization exclusively in growth cones. The Pearson's r is considered significant when its value is between 0.5 and 1. Thus we found that pERM-DCC colocalization was only significant after 5 min of netrin-1 stimulation ($r = 0.55 \pm 0.03$) compared with 20 min of stimulation ($r = 0.44 \pm 0.13$) or with unstimulated growth cones ($r = 0.38 \pm 0.03$) (Figure 5C). Of interest, inhibition of RhoA and Rho kinase by toxin B, C3 transferase, or Y27632 also abolished the accumulation of pERM in the growth cones (Figure 6 and Supplemental Figure S3). Therefore these results are in good agreement with the observation that netrin-1 transiently induces the interaction of ezrin with DCC in cortical neurons (Figure 2E) and demonstrate that netrin-1 induces the accumulation of pERM in growth cone filopodia where they interact with DCC, in a RhoA/Rho kinase–dependent manner.

Impairing ERM activity inhibits netrin-1–mediated axon outgrowth

The expression of DCC in N1E-115 cells induces neurite outgrowth (Figure 7, A and C) and was previously shown to occur in a netrin-1–dependent manner (Li *et al.*, 2002). To assess whether ezrin also induces neurite outgrowth in these cells, various ezrin protein mutants were expressed (Figure 7B). The expression of wild-type ezrin (ezrinWT) or constitutively active ezrinT567D (ezrinTD) induced a significant increase in neurite outgrowth compared with the empty vector control (Figure 7, B and C). Although the overexpression of ezrinWT or ezrinTD promoted neurite outgrowth in N1E-115 cells, the morphology of these neurites was different from those observed with DCC overexpression (Figure 7A). EzrinWT overexpression was associated with shorter neurites, and cells expressing ezrinTD exhibited more neuritic branching (Figure 7B). However, expression of ezrinT567A (ezrinTA), which keeps ezrin in its inactive conformation, or ezrinΔ29, in which the F-actin–binding domain is deleted (Figure 1B), did not induce neurite outgrowth in N1E-115 cells (Figure 7, B and C). The impact of ERM activity in DCC-mediated neurite outgrowth was then assessed by coexpressing DCC and ezrin protein mutants in neuroblastoma cells. The expression of the inactive protein mutant ezrinTA or ezrinΔ29 significantly inhibited DCC-induced neurite outgrowth (Figure 7C). However, the percentage of transfected cells exhibiting neurite outgrowth was not altered when ezrinWT or ezrinTD was coexpressed with DCC (Figure 7C). Therefore we conclude that ezrin is able to promote the extension of neurites in N1E-115 cells and that its activity is required for DCC-dependent neurite outgrowth.

Because netrin-1 induces axon outgrowth in cortical neurons (Liu *et al.*, 2004; Briancon-Marjollet *et al.*, 2008), we examined the impact of ERM proteins on netrin-1–induced axon outgrowth in embryonic cortical neurons. Dominant-negative ezrinΔ29 (EzΔ29) (D'Angelo *et al.*, 2007), wild-type ezrin (EzWT), or a green

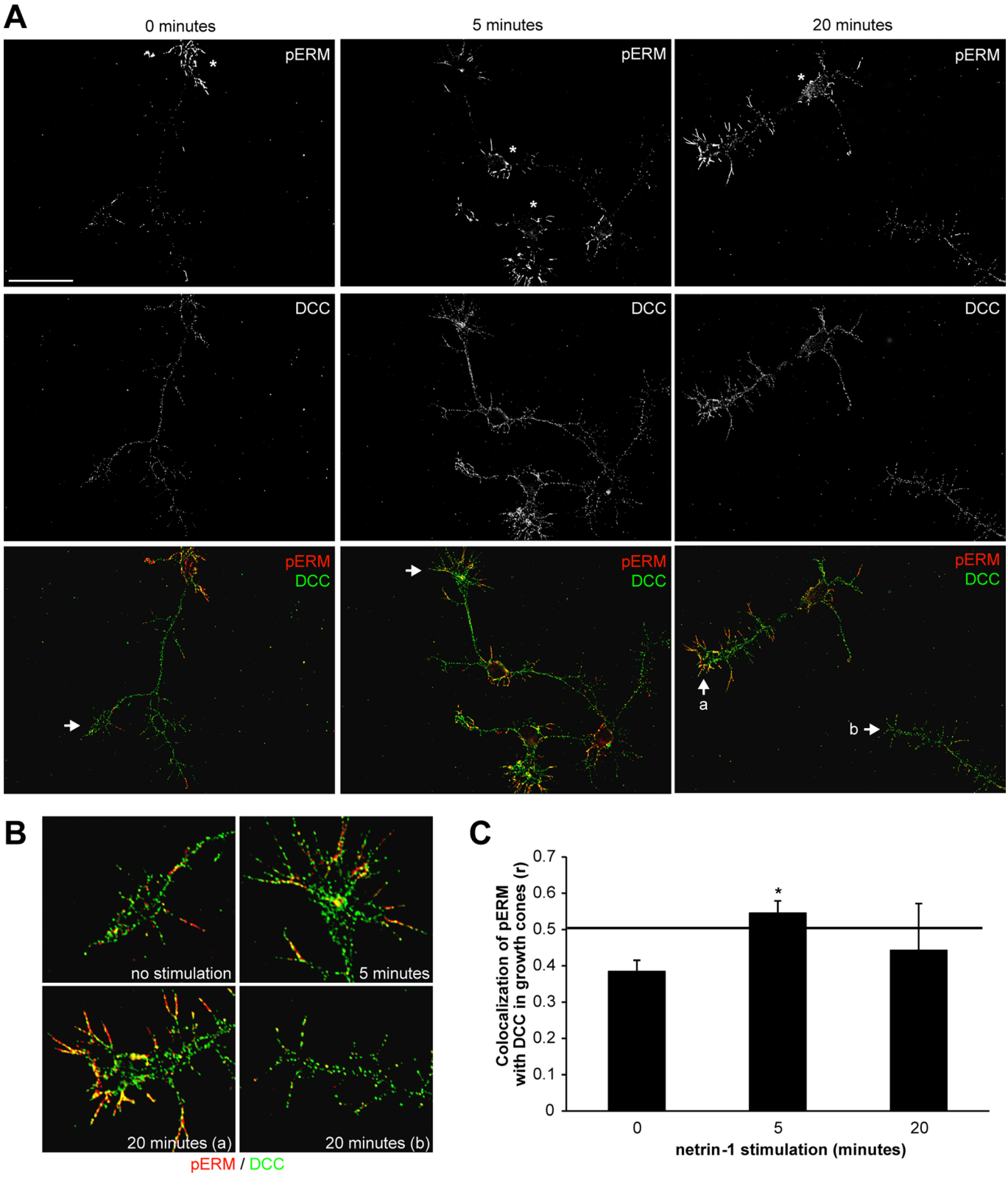

FIGURE 5: Netrin-1 induces the accumulation of phosphorylated ERM proteins and their colocalization with DCC in growth cone filopodia. (A) Embryonic rat cortical neurons (E18, 2DIV) were incubated with netrin-1 for the indicated times, fixed, and immunostained with antibodies against DCC (green) and pERM (red). Cell bodies are represented by asterisks. Scale bar, 5 μm. (B) Magnification of regions designated by arrows in A. Growth cones after 20 min of netrin-1 stimulation (a) with pERM-DCC colocalization, and (b) with no significant pERM-DCC colocalization. (C) Quantification of pERM–DCC colocalization in growth cones using Pearson's correlation coefficient r; *$p < 0.05$. The minimal r value for significant pERM-DCC colocalization is 0.5 (horizontal line). Error bars, SEM.

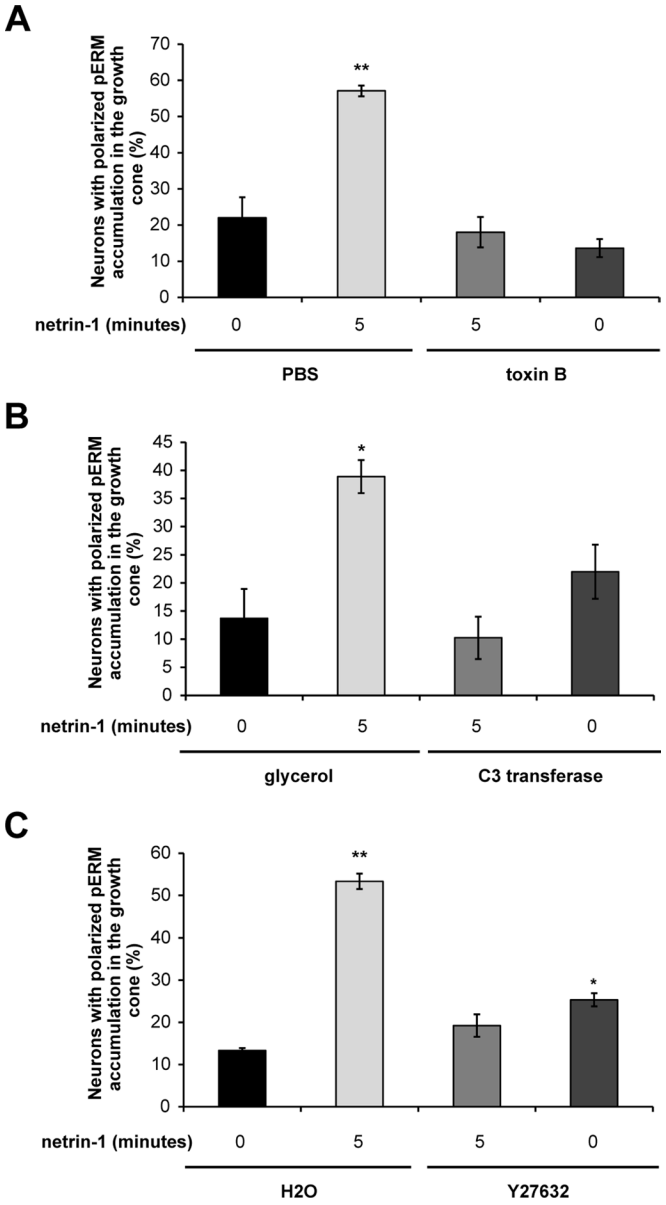

FIGURE 6: RhoA/Rho kinase is required to mediate the accumulation of phosphorylated ERM proteins in growth cones upon netrin-1 stimulation. Embryonic rat cortical neurons (E18, 2DIV) were incubated with netrin-1 for the indicated times following treatment with (A) Rho GTPase inhibitor toxin B or PBS as a negative control, (B) RhoA inhibitor C3 transferase (C3T) or glycerol as a negative control, or (C) Rho kinase inhibitor Y27632 or water (H_2O) as a negative control. Neurons were fixed and immunostained with anti-pERM and anti-DCC antibodies (Supplemental Figure S3). The quantification of the accumulation of phosphorylated ERM proteins (pERM) in growth cones corresponds to three independent experiments. Student's unpaired *t* test was used for statistical analysis, and the data are presented as mean percentage ± SEM (*$p < 0.05$; **$p < 0.005$).

fluorescent protein (GFP) control was expressed in neurons stimulated with netrin-1 for 24 h. Axon outgrowth was quantified as the percentage of transfected neurons that exhibit an axon longer than 35 µm over that of the control medium incubation (Figure 8). Netrin-1 did induce significant axon outgrowth in cortical neurons expressing GFP (Figure 8, A and B). However, it failed to promote axon outgrowth in neurons expressing ezrinΔ29, whereas the expression of ezrinWT did not affect the ability of netrin-1 to induce axon extension (Figure 8, A and B). In addition, down-regulation of ezrin expression by electroporation of synthetic siRNA targeting ezrin was sufficient to abolish the ability of netrin-1 to induce axon outgrowth (Figure 8, C and D). We previously reported that glutamate stimulation induces axon outgrowth in embryonic cortical neurons (Briancon-Marjollet *et al.*, 2008). Similarly, we observed that glutamate was capable of inducing axon outgrowth, but the expression of ezrinΔ29 significantly impaired its ability to promote axon outgrowth in cortical neurons (Figure 8B). Collectively, these results reveal an important role for ezrin in mediating the effects of netrin-1/DCC signaling on axon extension. The implication of ERM proteins in glutamate-induced axon outgrowth also suggests that ERM proteins play a more general role in axon outgrowth, which consists of coupling surface receptors to their downstream functions in response to extracellular cues.

DISCUSSION

In this study, we provide evidence that the axon guidance cue netrin-1 transiently induces ERM phosphorylation and promotes the interaction of ezrin with DCC in embryonic cortical neurons. We show that netrin-1 induces the accumulation of pERM in filopodial protrusions and colocalization with DCC at the extremities of neuronal growth cones. Moreover, our findings demonstrate that ezrin is required for netrin-1 to induce axon outgrowth in primary cortical neurons. The interaction between DCC and ezrin has previously been described in vitro and in colonic cancer cells (Martin *et al.*, 2006; Tcherkezian *et al.*, 2010). The intracellular domain of DCC harbors a juxtamembrane ERM-binding region, and its deletion prevented in vitro recruitment of FERM domains (ezrin and merlin) (Martin *et al.*, 2006). We also confirmed that the cytoplasmic tail of DCC is required to mediate the interaction DCC–ezrin in response to netrin-1 stimulation. Our proteomic data also reveal that the phosphorylation of the tyrosine residue 1418 positively regulates the interaction of ERM proteins with a phosphopeptide corresponding to the C-terminus of DCC in vitro. This is in good agreement with the finding that the C-terminus of DCC mediates the interaction with the FERM-containing protein myosin X (Zhu *et al.*, 2007). Thus both the juxtamembrane region and the C-terminus of DCC are implicated in the recruitment of ERM proteins to DCC, and our results suggest that phosphorylation of Y1418 is a regulatory step that promotes ERM–DCC complex formation in response to netrin-1 stimulation.

It is well established that the intramolecular interaction between the FERM domain and the C-terminus of ERM proteins inhibits their function (Berryman *et al.*, 1995; Pearson *et al.*, 2000). The affinity of the FERM domain for phosphatidylinositol 4,5 bisphosphate recruits ERM proteins to the plasma membrane (Barret *et al.*, 2000). Subsequently, phosphorylation of their conserved C-terminal threonine residue releases the FERM and the actin-binding domains (Matsui *et al.*, 1998; Fievet *et al.*, 2004). The sequential activation of ERM proteins enables them to interact with both the plasma membrane and the actin cytoskeleton. Recent findings showed that the extracellular cues Sema3A, NGF, and glutamate regulate ERM phosphorylation in neuronal cells (Mintz *et al.*, 2008; Jeon *et al.*, 2010; Kim *et al.*, 2010). Here we demonstrate that netrin-1 increases ERM phosphorylation in a DCC-dependent manner in primary cortical neurons. Of note, the formation of the ezrin–DCC protein complex and ERM phosphorylation occur in parallel and peak after 5 min of netrin-1 stimulation. Unlike the ezrin–DCC interaction, which was not detected past 5 min of netrin-1 stimulation, ERM phosphorylation decreases but appears to be maintained. This suggests that netrin-1 regulates the interaction in time and space by restricting the pool of ezrin that can interact with DCC. We also show that Src

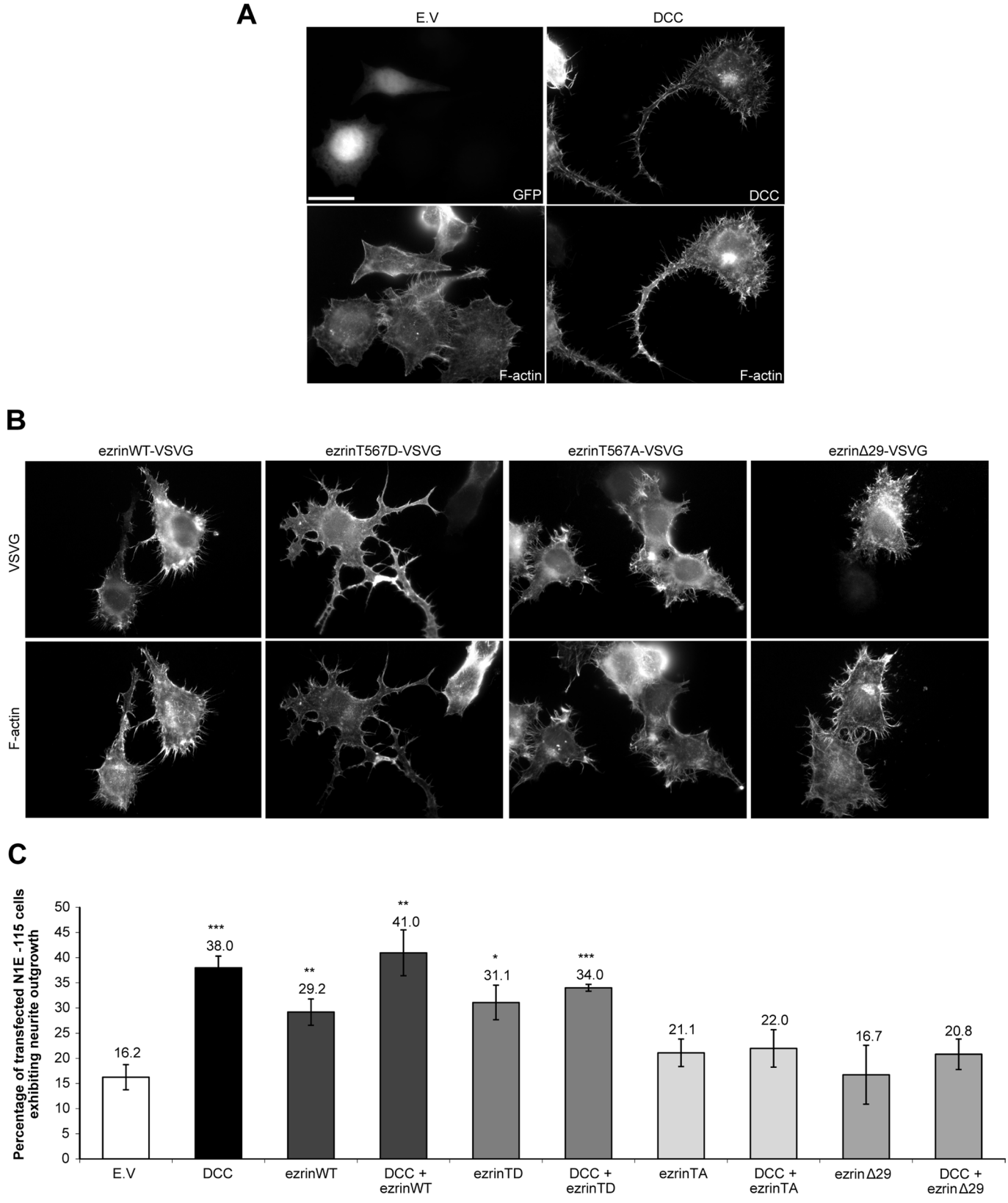

FIGURE 7: Impaired ezrin activity inhibits DCC-mediated neurite outgrowth. (A, B) N1E-115 cells were transfected with either pEGFP (E.V.), pRK5-DCC, pCB6-ezrin-VSVG (ezrinWT), pCB6-ezrinT567D-VSVG (ezrinTD), pCB6-ezrinT567A-VSVG (ezrinTA), or pCB6-ezrinΔ29-VSVG (ezrinΔ29), fixed, and immunostained with antibodies against DCC or VSVG. F-Actin was labeled with phalloidin-TRITC. Scale bar, 5 μm. (C) The percentage of transfected N1E-115 cells with neurites longer than their cell body was measured 24 h posttransfection. The values correspond to the average of at least three independent experiments in which at least 150 transfected cells were counted. Error bars, SEM (*$p < 0.05$; **$p < 0.01$; ***$p < 0.001$).

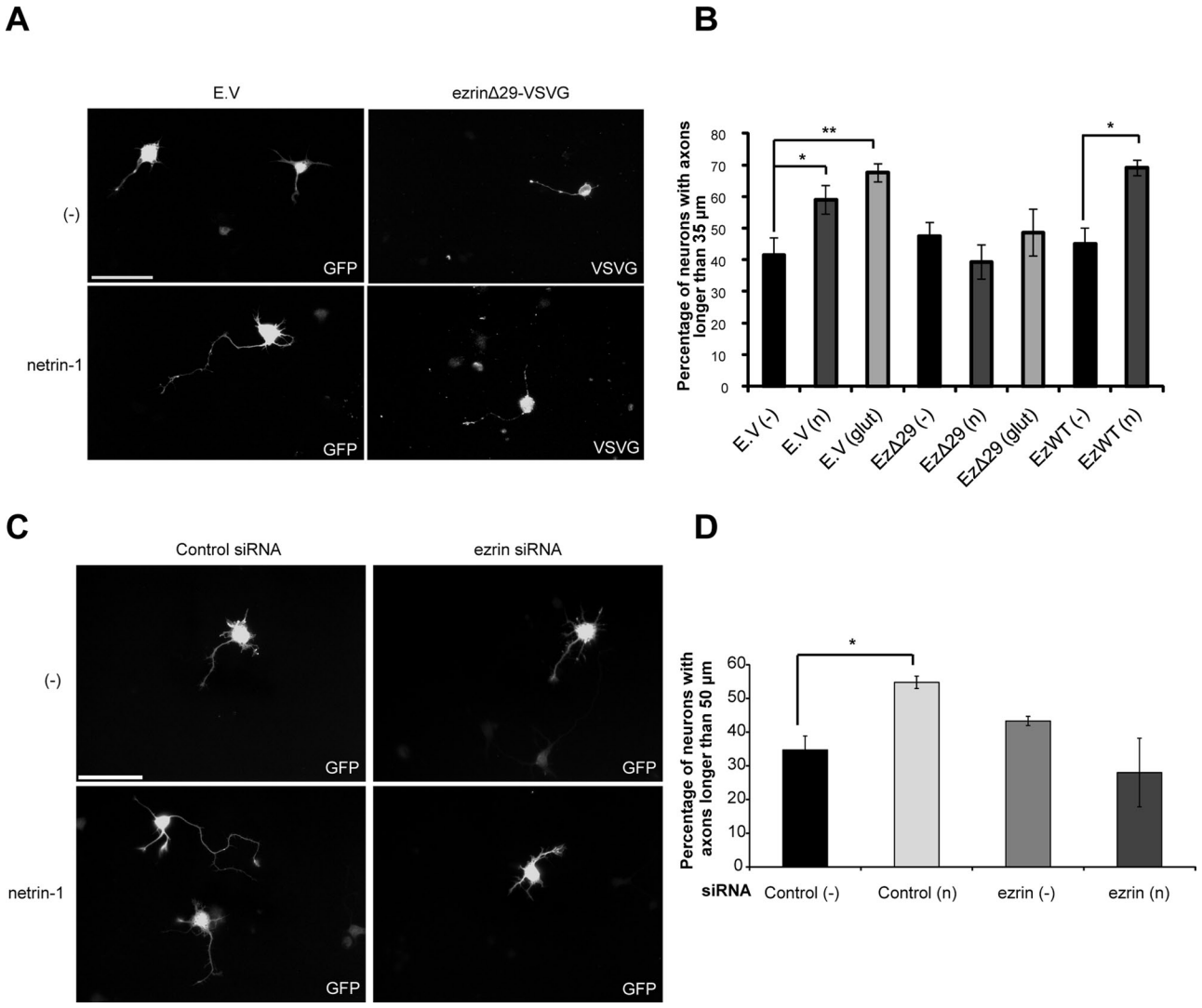

FIGURE 8: Dominant-negative ezrin and ezrin down-regulation inhibit netrin-1–mediated axon outgrowth. (A, B) Embryonic rat cortical neurons (E18) were transfected at 1DIV with pEGFP (empty vector, E.V.), pCB6-ezrin-VSVG (ezWT), or pCB6-ezrinΔ29-VSVG (ezΔ29) and incubated for 24 h with netrin-1 or control medium. Neurons were fixed at 2DIV and immunostained with anti-VSVG antibodies. (C, D) Embryonic rat cortical neurons (E18) were electroporated at 0DIV with pmaxGFP and Negative Control siRNA or with pmaxGFP and ezrin siRNA to down-regulate ezrin (Supplemental Figure S2, B and C) and incubated for 24 h with netrin-1 or control medium. Quantification of axon outgrowth in transfected cells following a 24-h incubation with control medium (–), netrin-1 (n), or glutamate (glut) is represented as the percentage of transfected cortical neurons with axons longer than 35 µm (B) or 50 µm (D) in length. The values correspond to the average of at least three independent experiments. Error bars, SEM (*$p < 0.05$; **$p < 0.001$). Scale bar, 50 µm.

kinase activity is required for netrin-1–induced ERM phosphorylation in cortical neurons. Src family kinases mediate tyrosine phosphorylation of DCC in response to netrin-1, which is essential for promoting netrin-1–dependent functions such as axon outgrowth and guidance in vertebrates (Li *et al.*, 2004; Meriane *et al.*, 2004; Ren *et al.*, 2008). Furthermore, the expression of a phospho-deficient mutant DCC-Y1418F was shown to inhibit Rac1 activation in COS-7 cells, neurite outgrowth in N1E-115 cells, and axon turning of *Xenopus* commissural neurons (Li *et al.*, 2004; Meriane *et al.*, 2004; Ren *et al.*, 2008). We provide further evidence of the significance of Y1418 phosphorylation in netrin-1 signaling by demonstrating that DCC expression increases ERM phosphorylation in N1E-115 cells, whereas DCC-Y1418F inhibits it. Taken together, these results reveal that Src kinase–dependent tyrosine phosphorylation of DCC mediates ERM activation in cortical neurons stimulated with netrin-1.

We found that inhibiting RhoA, Rac1, and Cdc42 with toxin B blocks netrin-1–dependent ERM phosphorylation in cortical neurons. Rho GTPases are regulated by netrin-1 and DCC in neuronal cells (Li *et al.*, 2002; Shekarabi and Kennedy, 2002; Moore *et al.*, 2008; Picard *et al.*, 2009). In addition, they have also been implicated in ERM activation in neuronal cells. Indeed, RhoA and Rho kinase promote ERM phosphorylation in cortical and hippocampal neurons (Haas *et al.*, 2007; Kim *et al.*, 2010). A recent study also implicates the positive regulation of Akt-dependent moesin phosphorylation by Rac1 in PC12 cells (Jeon *et al.*, 2010). Although it was reported that active Cdc42 promotes pERM accumulation in fibroblasts (Nakamura *et al.*, 2000), its role in ERM activation in neurons

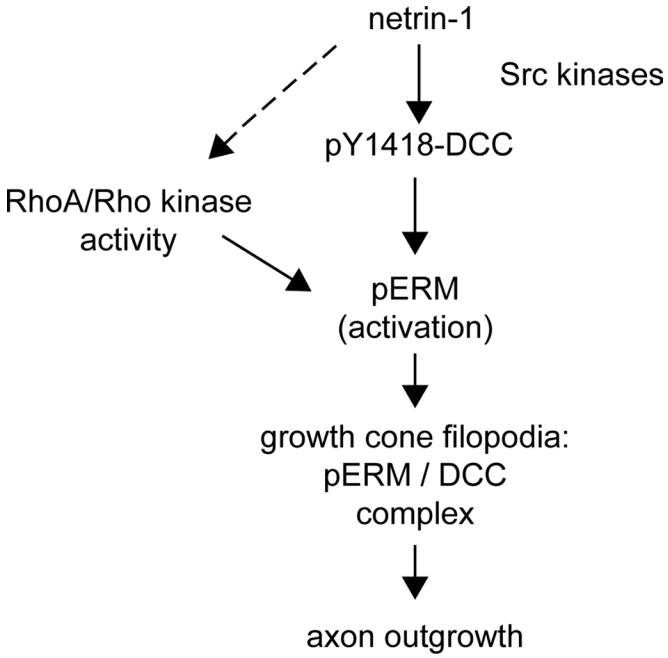

FIGURE 9: Regulation and function of the ERM–DCC complex downstream of netrin-1 in cortical neurons. Netrin-1 promotes tyrosine phosphorylation of DCC via Src kinases. The signaling cascade downstream of netrin-1 and its phosphorylated receptor promotes the phosphorylation of ERM protein in concert with RhoA and its effector, Rho kinase. The mechanism by which netrin-1 activates RhoA has yet to be determined (dashed arrow). Upon phosphorylation, activated ERM proteins (pERM) accumulate in growth cone filopodia, where they form a complex with DCC. The phosphorylation of the receptor on Y1418 positively regulates ERM protein activation, thus promoting ERM–DCC complex assembly. Ultimately, the activity of ERM proteins promotes axon outgrowth downstream of netrin-1, likely through their interaction with both DCC and the actin cytoskeleton in growth cone filopodia.

has yet to be defined. Our data reveal that inhibiting both Rac1 and Cdc42 does not decrease netrin-1–induced ERM phosphorylation, whereas RhoA and Rho kinase activities are required for netrin-1 to increase ERM phosphorylation in cortical neurons. Of interest, Moore *et al.* (2008) reported that netrin-1 induces whole-cell inhibition of RhoA activity in spinal commissural neurons and that prolonged RhoA inhibition promotes DCC-dependent axon outgrowth induced by netrin-1. Yet we find that RhoA/Rho kinase activity mediates the initial and short-lived peak in netrin-1–dependent ERM phosphorylation. Moreover, we previously showed that DCC is able to locally activate RhoA in neurites, using fluorescence resonance energy transfer intermolecular probes (Picard *et al.*, 2009), suggesting that a spatial and temporal regulation of RhoA would be a required step for netrin-1/DCC to mediate ERM activation during axon extension. Without contradicting previous reports, our study offers new insight into the regulation of RhoA activity by netrin-1. We propose that RhoA signaling is regulated by netrin-1 in at least two different ways: 1) short-term local activation to mediate ERM phosphorylation, and 2) long-term global inhibition to promote axon outgrowth.

Once they are phosphorylated, activated ERM proteins have been shown to localize to plasma membrane protrusions such as microvilli in nonneuronal cells (Yonemura *et al.*, 2002) and growth cone filopodia in neurons, where they are asymmetrically distributed (Haas *et al.*, 2004, 2007; Mintz *et al.*, 2008). Consistent with this, we found that netrin-1 stimulation of cortical neurons leads to the accumulation of pERM in growth cone filopodia, where they colocalize with DCC, in a RhoA/Rho kinase-dependent manner. This suggests that activated ERM proteins localize to growth cones to mediate netrin-1–dependent functions. Both netrin-1 and Sema3A regulate the endocytosis of their respective receptors, DCC and Npn1, in growth cones (Piper *et al.*, 2005). In parallel, ERM protein activity was reported to mediate Sema3A-induced growth cone collapse by regulating the internalization of Npn1 and L1 (Mintz *et al.*, 2008). This highlights the interesting possibility that ERM proteins may regulate the internalization of DCC in response to netrin-1.

We show that the activity of ERM proteins is required for axon outgrowth induced by netrin-1 and DCC. In a separate study, A. K. Howe *et al.* (unpublished data) found that DCC forms a complex with ezrin and protein kinase A (PKA). Of interest, they observed that silencing the expression of ezrin in rat hippocampal neurons impairs axon turning in response to netrin-1. Furthermore, down-regulation of ERM expression in IMR-32 cells blocks netrin-1–induced PKA activation and phosphorylation of its cytoskeletal targets VASP/MENA (A. K. Howe *et al.*, unpublished data). Given that ERM proteins are actin-binding proteins, loss of ERM activity in hippocampal and dorsal root ganglia neurons reduces filopodial dynamics in growth cones (Paglini *et al.*, 1998; Gallo, 2008). Consequently, the inhibition of protrusive activity due to the loss of ERM expression severely impairs neurite outgrowth and axonal extension in hippocampal neurons (Paglini *et al.*, 1998). Filopodial protrusions are also positively regulated by netrin-1 in cortical neurons, whereas the axon guidance cue Sema3A has an inhibitory effect (Dent *et al.*, 2004). These data and those presented in our study support burgeoning evidence that ERM activation in neuronal growth cones promotes axon outgrowth by regulating filopodial dynamics. The transmembrane receptors L1, CHL1, and Fas have also been reported to mediate neurite branching through ERM proteins (Cheng *et al.*, 2005; Ruan *et al.*, 2008; Schlatter *et al.*, 2008). We found that ERM protein activity is also required for glutamate-induced axon outgrowth in cortical neurons, which confirms that the role of ERM proteins in axon outgrowth is not exclusive to netrin-1. Here we propose a model in which netrin-1 promotes the phosphorylation of DCC and ERM proteins in a Src kinase and RhoA/Rho kinase–dependent manner to positively regulate their interaction in growth cone filopodia, leading to axon outgrowth (Figure 9). In conclusion, this study contributes to our knowledge of netrin-1/DCC signal transduction by providing novel insight into the regulation and the function of actin cytoskeleton regulators in the context of axon outgrowth.

MATERIALS AND METHODS

Plasmids

The plasmids pRK5, pRK5-DCC, pRK5-DCC-Y1418F, and pEGFP were previously described (Li *et al.*, 2002; Meriane *et al.*, 2004). pRK5-DCC (1-1120) was previously described (Tcherkezian *et al.*, 2010). For ezrin constructs, mammalian expression plasmids (pCB6-ezrin-VSVG, pCB6-ezrinT567D-VSVG, pCB6-ezrinT567A-VSVG, pCB6-ezrinΔ29-VSVG) and the plasmids encoding GST, GST-ezrin, and GST-ezrinNT were kindly provided by M. Arpin (Institut Curie, Paris, France) and previously described (Algrain *et al.*, 1993; Gautreau *et al.*, 1999, 2000; D'Angelo *et al.*, 2007).

Cell culture and transfection

Cell culture was maintained in a humidified incubator at 37°C with 5% CO_2. HEK293 cells and N1E-115 cells were cultured in DMEM (Wisent Bioproducts, St. Bruno, Canada) supplemented with 10% fetal bovine serum and antibiotics. N1E-115 cells were plated on dishes treated with laminin (25 μg/ml; BD Biosciences, San Diego, CA). Cells were transfected overnight with pRK5, pRK5-DCC,

pRK5-DCC (1-1120), pCB6-ezrin-VSVG, pCB6-ezrinΔ29-VSVG, or pCB6-ezrinT567D-VSVG using polyethylenimine (PEI; PolySciences, Warrington, PA) prepared according to the manufacturer's instructions. Briefly, HEK293 cells and N1E-115 cells were plated in 100-mm dishes and transfected when they reached 70–80% of confluency. cDNA constructs (5 μg) were incubated with PEI (30 μg) in 1 ml of DMEM for 15 min. The transfection mixes were then added to cells with 9 ml of fresh supplemented DMEM. For the neurite outgrowth assay, N1E-115 cells were plated in 35-mm dishes at a cell density of 1.25×10^6 on laminin-treated coverslips. The next day, cells were transfected with pRK5, pRK5-DCC, pCB6-ezrin-VSVG, pCB6-ezrinT567D-VSVG, pCB6-ezrinT567A-VSVG, or pCB6-ezrinΔ29-VSVG using Lipofectamine 2000 reagent (Invitrogen, Carlsbad, CA) according to the manufacturer's instructions.

Primary cortical neuron culture, transfection, and electroporation

Cortical neurons from E18 rat embryos were dissociated mechanically and plated on dishes treated with poly-D-lysine (0.1 mg/ml; Sigma-Aldrich, St. Louis, MO). Neurons were cultured overnight in attachment medium: MEM (Invitrogen) supplemented with 1 mM sodium pyruvate (Invitrogen), 0.6% D-glucose (Sigma-Aldrich), and 10% horse serum. The medium was replaced the next day with maintenance medium: Neurobasal-A medium (Invitrogen) supplemented with 2% B27 (Invitrogen) and 1% L-glutamine (Invitrogen). For transfections, dissociated neurons were plated on coverslips treated with poly-L-lysine (0.1 mg/ml; Sigma-Aldrich) at a cell density of 75,000 cells/well in 24-well dishes. Neurons were cultured for 6 h in attachment medium. The medium was then replaced overnight with maintenance medium. Neurons were transfected at 1DIV for 24 h with pEGFP, pCB6-ezrin-VSVG, or pCB6-ezrinΔ29-VSVG using Lipofectamine 2000 reagent according to the manufacturer's instructions. Neurons were treated for the indicated times with the following reagents: purified myc-netrin-1 (500 ng/ml), glutamate (50 μM), generously provided by D. Bowie (McGill University, Montreal, Canada), function-blocking anti-DCC (AF5) antibody (5 μg/ml for 24 h; Calbiochem, La Jolla, CA), ImmunoPure mouse IgG (5 μg/ml for 24 h; Pierce, Thermo Fisher Scientific, Rockford, IL), PP2 (10 μM overnight; Calbiochem), toxin B (1 ng/ml for 24 h) previously described (Li *et al*., 2002), C3 transferase (1 μg/ml for 6 h; Cytoskeleton, Denver, CO), NSC23766 (100 μM for 2 h; Calbiochem), Y27632 (20 μM for 6 h; Calbiochem), DMSO (Thermo Fisher Scientific), and glycerol (Thermo Fisher Scientific). Recombinant chick netrin-1 was produced and purified as previously described (Serafini *et al*., 1994). The Amaxa Rat Neuron Nucleofector Kit (Lonza, Basel, Switzerland) was used to introduce 300 nM of synthetic ezrin siRNA (ON-TARGETplus SMARTpool, Thermo Fisher Scientific), Cdc42 siRNA (Silencer Select; Applied Biosystems/Ambion, Austin, TX), or Negative Control siRNA (Silencer #1; Applied Biosystems/Ambion) with or without 2 μg of pmaxGFP Vector (Lonza) in cortical neurons as per the manufacturer's instruction.

Antibodies

The following antibodies were used for immunoblotting and immunofluorescence at the indicated concentrations: mouse monoclonal anti-DCC, clone G97-449 (BD Biosciences), 1:4000 (immunoblot; IB) and 1:500 (immunofluorescence, IF); mouse monoclonal (AF5) anti-DCC (Calbiochem), 1:1000 (IB); mouse anti-actin (Sigma-Aldrich), 1:2000 (IB); rabbit polyclonal anti-ezrin (kindly provided by M. Arpin; Algrain *et al*., 1993), 1:7000 (IB) and 1:500 (IF); mouse monoclonal anti-VSVG (Sigma-Aldrich), 1:40,000 (IB) and 1:300 (IF); rabbit monoclonal anti-pERM (ezrin [Thr-567]/radixin [Thr-564]/moesin [Thr-558]); Cell Signaling Technology, Beverly, MA), 1:1000 (IB) and 1:300 (IF); rabbit polyclonal anti-Cdc42 (Cell Signaling Technology), 1:500 (IB); donkey anti–mouse Alexa 488 (Molecular Probes, Invitrogen), 1:1000 (IF); and goat anti–rabbit tetramethyl rhodamine isothiocyanate (TRITC; Sigma-Aldrich), 1:500 (IF).

Affinity purification and mass spectrometry

An affinity column was prepared using a phosphopeptide corresponding to amino acids 1409–1423 of rat DCC (Small Scale Peptide Synthesis, W. M. Keck Facility, Yale University, New Haven, CT), phosphorylated on tyrosine 1418 (KPTEDPASVpYEQDDL) coupled to Affi-Gel (Bio-Rad, Hercules, CA) according to the manufacturer's protocol. An unphosphorylated peptide and Affi-Gel beads were used as negative controls. Protein lysates from E13 rat brains were loaded on each column, and proteins bound to the affinity columns were eluted using a gradient of sodium chloride by fast protein liquid chromatography. The eluted proteins were separated by SDS–PAGE, and proteins were detected using the Coomassie blue gel staining method. An 85-kDa band that was present only in the phosphopeptide affinity purification was cut and sent to be identified by tandem mass spectrometry. Protein identification was made with Mascot software (Matrix Science, Boston, MA).

GST pull-down

Recombinant GST proteins were purified as described (Gautreau *et al*., 1999). Transfected HEK293 cells were lysed in 1% Triton X-100 lysis buffer (25 mM Tris-HCl, pH 7.5, 1% Triton X-100, 10 mM NaCl, 1 mM EDTA, 1 mM phenylmethylsulfonyl fluoride, 1 mM Na_2VO_4, 20 mM NaF, and 1× Complete Protease Inhibitor Cocktail [Roche, Indianapolis, IN]). Lysates were precleared with 30 μl of glutathione–agarose beads (Sigma Aldrich) for 2 h at 4°C and then incubated with 10 μg of GST, GST-ezrin, or GST-ezrinNT fusion proteins coupled to glutathione–agarose beads for 3 h at 4°C. Beads were washed three times in ice-cold lysis buffer and boiled in SDS sample buffer. Total cell lysates and GST pull-down–associated proteins were resolved by SDS–PAGE and transferred onto nitrocellulose membrane. Membranes were stained with Ponceau S (Sigma-Aldrich), immunoblotted with antibodies against DCC, and visualized using enhanced chemiluminescence (ECL; PerkinElmer, Waltham, MA).

RT-PCR

mRNA was extracted from purified total RNA obtained from homogenized cortices or dissociated cortical neurons in culture (1, 2, and 3DIV) using the QIAshredder homogenizer and RNeasy Mini kits (Qiagen, Valencia, CA) according to the manufacturer's protocol. First-strand cDNA was synthesized using M-MLV reverse transcriptase (Invitrogen). The Expand High Fidelity PCR system (Roche) was used to amplify cDNA fragments (sizes are indicated) using the following forward and reverse primers: ezrin, GGAGGTTCGAAAGGAGAACC and ACCCAGACTTGTGCATTTCC, 233 base pairs; moesin, TGGTCCAGGAAGACTTGGAG and TGCACACGCTCATTCTTCTC, 205 base pairs; radixin, CTCCATGCTGAGAACGTCAA and CCTCGGGTTCTGCTAGTGAG, 242 base pairs; merlin, TGCTATGCCTCAGTCCACAG and TGCTGAGGTGTCAAGTCCTG, 248 base pairs; glyceraldehyde-3-phosphate dehydrogenase (GAPDH), AGACAGCCGCATCTTCTTGT and CTTGCCGTGGGTAGAGTCAT, 207 base pairs. The primers were annealed at 55°C, and 30 cycles were carried out.

Immunoprecipitations and immunoblotting

Dissociated cortical neurons (2DIV) and transfected N1E-115 cells were lysed in RIPA lysis buffer (150 mM NaCl, 50 mM 4-(2-hydroxyethyl)-1-piperazineethanesulfonic acid, pH 7.5, 1% NP-40, 10 mM EDTA,

pH 8.0, 0.5% sodium deoxycholate, 0.1% SDS). Prior to cell lysis, cortical neurons were incubated with netrin-1 or control Neurobasal-A media. For immunoprecipitation, 1 mg of protein lysates was incubated with 20 µl of protein G–Sepharose (GE Healthcare, Piscataway, NJ) and 1.5 µg of anti-DCC antibodies (Calbiochem) or mouse IgG for 3 h at 4°C. Beads were washed three times in ice-cold lysis buffer and boiled in SDS sample buffer. Immunoprecipitated proteins and total cell lysates were resolved by SDS–PAGE and transferred to nitrocellulose membrane for immunoblotting with the appropriate antibodies and visualized by enhanced chemiluminescence.

Quantitative densitometry of ERM phosphorylation and of Cdc42 and ezrin down-regulation

Following treatment with the indicated reagents, treated and untreated dissociated cortical neurons (2DIV) were lysed in RIPA buffer following incubation with netrin-1 or control media. Protein lysates were resolved by SDS–PAGE and transferred to nitrocellulose for immunoblotting with anti-pERM, anti-ezrin, anti-Cdc42, and anti-actin antibodies. Quantitative densitometry for pERM, ezrin, Cdc42, and actin bands was measured using Quantity One software (Bio-Rad). The ratio of the densitometry of pERM over that of total ezrin, of Cdc42 over that of actin, and of ezrin over that of actin was then calculated. Student's unpaired *t* test was used for statistical analysis, and the data are presented as the mean of the pERM/ezrin, Cdc42/actin, or ezrin/actin ratio ± standard error of the mean (SEM).

Immunofluorescence and microscopy

Transfected N1E-115 cells and dissociated cortical neurons (2DIV) were fixed with 3.7% formaldehyde in phosphate-buffered saline (PBS) for 15 min, quenched in 0.1 M glycine for 5 min, permeabilized in 0.25% Triton X-100 for 5 min, and blocked with 0.2 or 10% bovine serum albumin (BSA) for 30 min, respectively. N1E-115 cells and cortical neurons were immunostained with primary (1 h) and secondary antibodies (45 min) in 0.2 or 3% BSA, respectively. A 5-min wash in PBS was done between each step. For the pERM and DCC coimmunostaining in dissociated cortical neurons (2DIV), the trichloroacetic acid fixation and staining methods described previously were used (Hayashi *et al*., 1999). Phalloidin-TRITC (1:5000, Sigma-Aldrich) was used to visualize actin in N1E-115 cells. Glass coverslips were mounted with Prolong (Molecular Probes). Cells were examined with an Olympus IX81 motorized inverted microscope using the 40× U PLAN Fluorite and 60× U PLAN S-APO oil objective lenses. Images were recorded with a CoolSnap 4K camera (Photometrics, Tucson, AZ) and analyzed with Metamorph software (Molecular Devices, Sunnyvale, CA).

Quantification of colocalization using Pearson's correlation coefficient and quantification of the accumulation of phosphorylated ERM proteins in growth cones

Dissociated cortical neurons were incubated with netrin-1 or control media at 2DIV, and immunofluorescence was performed. Images of the pERM and DCC coimmunostaining were acquired with the 60× objective lens and deconvoluted using AutoQuant X2 software (MediaCybernetics, Bethesda, MD). Pearson's correlation coefficient was then calculated for each set of images using Metamorph software. More than 50 growth cones per condition were analyzed in least three independent experiments. Student's unpaired *t* test was used for statistical analysis, and the data are presented as mean r ± SEM. The accumulation of pERM in growth cones was determined by analyzing more than 75 neurons in three independent experiments. Student's unpaired *t* test was used for statistical analysis, and the data are presented as mean percentage ± SEM.

Axon outgrowth assay

Two hours after transfection or 24 h after electroporation, netrin-1 (250 ng/ml), glutamate (50 µM), or control medium was added to dissociated cortical neurons at 1DIV. Immunofluorescence was performed 24 h after transfection. Images were acquired with the 40× objective lens, and the length of each axon was measured using Metamorph. Axon outgrowth was then represented as the percentage of neurons with axons longer than 35 or 50 µm after treatment with netrin-1 or glutamate over the percentage observed with control media for each transfection. More than 100 axons were counted per condition, and at least three independent experiments were performed. Student's unpaired *t* test was used for statistical analysis, and the data are presented as mean percentage ± SEM.

ACKNOWLEDGMENTS

We are grateful to Monique Arpin for providing cDNA constructs encoding ezrin proteins and the anti-ezrin antibody. We thank Ibtissem Triki, Line Roy, and the McGill University and Genome Quebec Innovation Centre for technical assistance and helpful discussions regarding the proteomic analysis. We also thank Alan Howe for helpful discussions and critical reading of the manuscript. This research was supported by Canadian Institute of Health Research Grant MOP-14701 and the Canada Foundation for Innovation-Leaders Opportunity Fund. N.L.V. is a recipient of a Fonds de la Recherche en Santé du Québec Chercheur-National.

REFERENCES

Algrain M, Turunen O, Vaheri A, Louvard D, Arpin M (1993). Ezrin contains cytoskeleton and membrane binding domains accounting for its proposed role as a membrane-cytoskeletal linker. J Cell Biol 120, 129–139.

Barret C, Roy C, Montcourrier P, Mangeat P, Niggli V (2000). Mutagenesis of the phosphatidylinositol 4,5-bisphosphate (PIP(2)) binding site in the NH(2)-terminal domain of ezrin correlates with its altered cellular distribution. J Cell Biol 151, 1067–1080.

Berryman M, Gary R, Bretscher A (1995). Ezrin oligomers are major cytoskeletal components of placental microvilli: a proposal for their involvement in cortical morphogenesis. J Cell Biol 131, 1231–1242.

Briancon-Marjollet A *et al*. (2008). Trio mediates netrin-1-induced Rac1 activation in axon outgrowth and guidance. Mol Cell Biol 28, 2314–2323.

Charrin S, Alcover A (2006). Role of ERM (ezrin-radixin-moesin) proteins in T lymphocyte polarization, immune synapse formation and in T cell receptor-mediated signaling. Front Biosci 11, 1987–1997.

Cheng L, Itoh K, Lemmon V (2005). L1-mediated branching is regulated by two ezrin-radixin-moesin (ERM)-binding sites, the RSLE region and a novel juxtamembrane ERM-binding region. J Neurosci 25, 395–403.

D'Angelo R, Aresta S, Blangy A, Del Maestro L, Louvard D, Arpin M (2007). Interaction of ezrin with the novel guanine nucleotide exchange factor PLEKHG6 promotes RhoG-dependent apical cytoskeleton rearrangements in epithelial cells. Mol Biol Cell 18, 4780–4793.

Dent EW, Barnes AM, Tang F, Kalil K (2004). Netrin-1 and semaphorin 3A promote or inhibit cortical axon branching, respectively, by reorganization of the cytoskeleton. J Neurosci 24, 3002–3012.

Fazeli A *et al*. (1997). Phenotype of mice lacking functional Deleted in Colorectal Cancer (DCC) gene. Nature 386, 796–804.

Fehon RG, McClatchey AI, Bretscher A (2010). Organizing the cell cortex: the role of ERM proteins. Nat Rev Mol Cell Biol 11, 276–287.

Fievet BT, Gautreau A, Roy C, Del Maestro L, Mangeat P, Louvard D, Arpin M (2004). Phosphoinositide binding and phosphorylation act sequentially in the activation mechanism of ezrin. J Cell Biol 164, 653–659.

Gallo G (2008). Semaphorin 3A inhibits ERM protein phosphorylation in growth cone filopodia through inactivation of PI3K. Dev Neurobiol 68, 926–933.

Gary R, Bretscher A (1995). Ezrin self-association involves binding of an N-terminal domain to a normally masked C-terminal domain that includes the F-actin binding site. Mol Biol Cell 6, 1061–1075.

Gautreau A, Louvard D, Arpin M (2000). Morphogenic effects of ezrin require a phosphorylation-induced transition from oligomers to monomers at the plasma membrane. J Cell Biol 150, 193–203.

Gautreau A, Poullet P, Louvard D, Arpin M (1999). Ezrin, a plasma membrane-microfilament linker, signals cell survival through the phosphatidylinositol 3-kinase/Akt pathway. Proc Natl Acad Sci USA 96, 7300–7305.
Govek EE, Newey SE, Van Aelst L (2005). The role of the Rho GTPases in neuronal development. Genes Dev 19, 1–49.
Guan KL, Rao Y (2003). Signalling mechanisms mediating neuronal responses to guidance cues. Nat Rev Neurosci 4, 941–956.
Haas MA, Vickers JC, Dickson TC (2004). Binding partners L1 cell adhesion molecule and the ezrin-radixin-moesin (ERM) proteins are involved in development and the regenerative response to injury of hippocampal and cortical neurons. Eur J Neurosci 20, 1436–1444.
Haas MA, Vickers JC, Dickson TC (2007). Rho kinase activates ezrin-radixin-moesin (ERM) proteins and mediates their function in cortical neuron growth, morphology and motility in vitro. J Neurosci Res 85, 34–46.
Hall A, Lalli G (2010). Rho and Ras GTPases in axon growth, guidance, and branching. Cold Spring Harb Perspect Biol 2, a001818.
Hayashi K, Yonemura S, Matsui T, Tsukita S (1999). Immunofluorescence detection of ezrin/radixin/moesin (ERM) proteins with their carboxyl-terminal threonine phosphorylated in cultured cells and tissues. J Cell Sci 112, 1149–1158.
Huber AB, Kolodkin AL, Ginty DD, Cloutier JF (2003). Signaling at the growth cone: ligand-receptor complexes and the control of axon growth and guidance. Annu Rev Neurosci 26, 509–563.
Jeon S, Park JK, Bae CD, Park J (2010). NGF-induced moesin phosphorylation is mediated by the PI3K, Rac1 and Akt and required for neurite formation in PC12 cells. Neurochem Int 56, 810–818.
Keino-Masu K, Masu M, Hinck L, Leonardo ED, Chan SS, Culotti JG, Tessier-Lavigne M (1996). Deleted in Colorectal Cancer (DCC) encodes a netrin receptor. Cell 87, 175–185.
Kennedy TE, Serafini T, de la Torre JR, Tessier-Lavigne M (1994). Netrins are diffusible chemotropic factors for commissural axons in the embryonic spinal cord. Cell 78, 425–435.
Kikuchi S, Hata M, Fukumoto K, Yamane Y, Matsui T, Tamura A, Yonemura S, Yamagishi H, Keppler D, Tsukita S (2002). Radixin deficiency causes conjugated hyperbilirubinemia with loss of Mrp2 from bile canalicular membranes. Nat Genet 31, 320–325.
Kim HS, Bae CD, Park J (2010). Glutamate receptor-mediated phosphorylation of ezrin/radixin/moesin proteins is implicated in filopodial protrusion of primary cultured hippocampal neuronal cells. J Neurochem 113, 1565–1576.
Li W, Lee J, Vikis HG, Lee SH, Liu G, Aurandt J, Shen TL, Fearon ER, Guan JL, Han M *et al.* (2004). Activation of FAK and Src are receptor-proximal events required for netrin signaling. Nat Neurosci 7, 1213–1221.
Li X, Saint-Cyr-Proulx E, Aktories K, Lamarche-Vane N (2002). Rac1 and Cdc42 but not RhoA or Rho kinase activities are required for neurite outgrowth induced by the Netrin-1 receptor DCC (Deleted in Colorectal Cancer) in N1E-115 neuroblastoma cells. J Biol Chem 277, 15207–15214.
Liu G, Beggs H, Jurgensen C, Park HT, Tang H, Gorski J, Jones KR, Reichardt LF, Wu J, Rao Y (2004). Netrin requires focal adhesion kinase and Src family kinases for axon outgrowth and attraction. Nat Neurosci 7, 1222–1232.
Lowery LA, Van Vactor D (2009). The trip of the tip: understanding the growth cone machinery. Nat Rev Mol Cell Biol 10, 332–343.
Marsick BM, Flynn KC, Santiago-Medina M, Bamburg JR, Letourneau PC (2010). Activation of ADF/cofilin mediates attractive growth cone turning toward nerve growth factor and netrin-1. Dev Neurobiol 70, 565–588.
Martin M, Simon-Assmann P, Kedinger M, Mangeat P, Real FX, Fabre M (2006). DCC regulates cell adhesion in human colon cancer derived HT-29 cells and associates with ezrin. Eur J Cell Biol 85, 769–783.
Matsui T, Maeda M, Doi Y, Yonemura S, Amano M, Kaibuchi K, Tsukita S (1998). Rho-kinase phosphorylates COOH-terminal threonines of ezrin/radixin/moesin (ERM) proteins and regulates their head-to-tail association. J Cell Biol 140, 647–657.
McClatchey AI, Fehon RG (2009). Merlin and the ERM proteins—regulators of receptor distribution and signaling at the cell cortex. Trends Cell Biol 19, 198–206.
Meriane M, Tcherkezian J, Webber CA, Danek EI, Triki I, McFarlane S, Bloch-Gallego E, Lamarche-Vane N (2004). Phosphorylation of DCC by Fyn mediates Netrin-1 signaling in growth cone guidance. J Cell Biol 167, 687–698.
Metin C, Deleglise D, Serafini T, Kennedy TE, Tessier-Lavigne M (1997). A role for netrin-1 in the guidance of cortical efferents. Development 124, 5063–5074.
Mintz CD, Carcea I, McNickle DG, Dickson TC, Ge Y, Salton SR, Benson DL (2008). ERM proteins regulate growth cone responses to Sema3A. J Comp Neurol 510, 351–366.
Moore SW, Correia JP, Lai Wing Sun K, Pool M, Fournier AE, Kennedy TE (2008). Rho inhibition recruits DCC to the neuronal plasma membrane and enhances axon chemoattraction to netrin 1. Development 135, 2855–2864.
Nakamura N, Oshiro N, Fukata Y, Amano M, Fukata M, Kuroda S, Matsuura Y, Leung T, Lim L, Kaibuchi K (2000). Phosphorylation of ERM proteins at filopodia induced by Cdc42. Genes Cells 5, 571–581.
Niggli V, Rossy J (2008). Ezrin/radixin/moesin: versatile controllers of signaling molecules and of the cortical cytoskeleton. Int J Biochem Cell Biol 40, 344–349.
O'Donnell M, Chance RK, Bashaw GJ (2009). Axon growth and guidance: receptor regulation and signal transduction. Annu Rev Neurosci 32, 383–412.
Paglini G, Kunda P, Quiroga S, Kosik K, Caceres A (1998). Suppression of radixin and moesin alters growth cone morphology, motility, and process formation in primary cultured neurons. J Cell Biol 143, 443–455.
Pearson MA, Reczek D, Bretscher A, Karplus PA (2000). Structure of the ERM protein moesin reveals the FERM domain fold masked by an extended actin binding tail domain. Cell 101, 259–270.
Picard M, Petrie RJ, Antoine-Bertrand J, Saint-Cyr-Proulx E, Villemure JF, Lamarche-Vane N (2009). Spatial and temporal activation of the small GTPases RhoA and Rac1 by the netrin-1 receptor UNC5a during neurite outgrowth. Cell Signal 21, 1961–1973.
Piper M, Salih S, Weinl C, Holt CE, Harris WA (2005). Endocytosis-dependent desensitization and protein synthesis-dependent resensitization in retinal growth cone adaptation. Nat Neurosci 8, 179–186.
Rajasekharan S, Kennedy TE (2009). The netrin protein family. Genome Biol 10, 239.
Ramesh V (2004). Merlin and the ERM proteins in Schwann cells, neurons and growth cones. Nat Rev Neurosci 5, 462–470.
Ren XR, Hong Y, Feng Z, Yang HM, Mei L, Xiong WC (2008). Tyrosine phosphorylation of netrin receptors in netrin-1 signaling. Neurosignals 16, 235–245.
Richards LJ, Koester SE, Tuttle R, O'Leary DD (1997). Directed growth of early cortical axons is influenced by a chemoattractant released from an intermediate target. J Neurosci 17, 2445–2458.
Ruan W, Lee CT, Desbarats J (2008). A novel juxtamembrane domain in tumor necrosis factor receptor superfamily molecules activates Rac1 and controls neurite growth. Mol Biol Cell 19, 3192–3202.
Saotome I, Curto M, McClatchey AI (2004). Ezrin is essential for epithelial organization and villus morphogenesis in the developing intestine. Dev Cell 6, 855–864.
Schlatter MC, Buhusi M, Wright AG, Maness PF (2008). CHL1 promotes Sema3A-induced growth cone collapse and neurite elaboration through a motif required for recruitment of ERM proteins to the plasma membrane. J Neurochem 104, 731–744.
Serafini T, Colamarino SA, Leonardo ED, Wang H, Beddington R, Skarnes WC, Tessier-Lavigne M (1996). Netrin-1 is required for commissural axon guidance in the developing vertebrate nervous system. Cell 87, 1001–1014.
Serafini T, Kennedy TE, Galko MJ, Mirzayan C, Jessell TM, Tessier-Lavigne M (1994). The netrins define a family of axon outgrowth-promoting proteins homologous to *C. elegans* UNC-6. Cell 78, 409–424.
Shekarabi M, Kennedy TE (2002). The netrin-1 receptor DCC promotes filopodia formation and cell spreading by activating Cdc42 and Rac1. Mol Cell Neurosci 19, 1–17.
Shekarabi M, Moore SW, Tritsch NX, Morris SJ, Bouchard JF, Kennedy TE (2005). Deleted in Colorectal Cancer binding netrin-1 mediates cell substrate adhesion and recruits Cdc42, Rac1, Pak1, and N-WASP into an intracellular signaling complex that promotes growth cone expansion. J Neurosci 25, 3132–3141.
Shu T, Valentino KM, Seaman C, Cooper HM, Richards LJ (2000). Expression of the netrin-1 receptor, Deleted in Colorectal Cancer (DCC), is largely confined to projecting neurons in the developing forebrain. J Comp Neurol 416, 201–212.
Tcherkezian J, Brittis PA, Thomas F, Roux PP, Flanagan JG (2010). Transmembrane receptor DCC associates with protein synthesis machinery and regulates translation. Cell 141, 632–644.
Yonemura S, Matsui T, Tsukita S (2002). Rho-dependent and -independent activation mechanisms of ezrin/radixin/moesin proteins: an essential role for polyphosphoinositides in vivo. J Cell Sci 115, 2569–2580.
Zhu XJ, Wang CZ, Dai PG, Xie Y, Song NN, Liu Y, Du QS, Mei L, Ding YQ, Xiong WC (2007). Myosin X regulates netrin receptors and functions in axonal path-finding. Nat Cell Biol 9, 184–192.